Bacteriorhodopsin (bR) as an electronic conduction medium: Current transport through bR-containing monolayers

Yongdong Jin*, Noga Friedman*, Mordechai Sheves*†, Tao He‡, and David Cahen†‡

Departments of *Organic Chemistry and ‡Materials and Interfaces, Weizmann Institute of Science, Rehovot 76100, Israel

Edited by Mostafa A. El-Sayed, Georgia Institute of Technology, Atlanta, GA, and approved April 19, 2006 (received for review December 28, 2005)

Studying electron transport (ET) through proteins is hampered by achieving reproducible experimental configurations, particularly electronic contacts to the proteins. The transmembrane protein bacteriorhodopsin (bR), a natural light-activated proton pump in purple membranes of *Halobacterium salinarum*, is well studied for biomolecular electronics because of its sturdiness over a wide range of conditions. To date, related studies of dry bR systems focused on photovoltage generation and photoconduction with multilayers, rather than on the ET ability of bR, which is understandable because ET across 5-nm-thick, apparently insulating membranes is not obvious. Here we show that electronic current passes through bR-containing artificial lipid bilayers in solid ''electrode–bilayer–electrode'' structures and that the current through the protein is more than four orders of magnitude higher than would be estimated for direct tunneling through 5-nm, water-free peptides. We find that ET occurs only if retinal or a close analogue is present in the protein. As long as the retinal can isomerize after light absorption, there is a photo-ET effect. The contribution of light-driven proton pumping to the steady-state photocurrents is negligible. Possible implications in view of the suggested early evolutionary origin of halobacteria are noted.

molecular electronics | vesicles | bioelectronics

Bacteriorhodopsin (bR) is a protein–chromophore complex that serves as a light-driven proton pump in the purple membrane (PM) of *Halobacterium salinarum* (1). It has been shown that the protein is composed of seven transmembrane helices with a retinal chromophore covalently bound in the central region via a protonated Schiff base to a lysine residue (Fig. 1*A*). The PM is organized in a 2D hexagonal crystal lattice with a unit cell dimension of ≈6.2 nm. Electron crystallography has indicated that bR is organized into trimers in which lipids mediate intertrimer contact (2). Light absorption by bR initiates a multistep reaction cycle with several distinct spectroscopic intermediates: J_{625}, K_{590}, L_{550}, M_{412}, N_{560}, and O_{640}. More details on the molecular alterations that occur during the photocycle were recently obtained from x-ray diffraction studies (see ref. 3 for a recent review). The light-adapted form of bR contains only *all-trans* retinal, whereas the dark-adapted form contains a 1:1 mixture of *13-cis* and *all-trans* (4). Because of its long-term stability against thermal, chemical, and photochemical degradation and its desirable photoelectric and photochromic properties, bR has attracted much interest as a material for biooptics and bioelectronics (5). Most of these efforts focused on multilayers and their photovoltage/photocurrent generation (6–8) and photoconduction (9).

In principle, PM patches (≈5 nm thick, a few μm in size; see Fig. 1*B*) can serve as a model protein material that is important for both planar junction fabrication and current transport measurements, because the 5-nm membrane is well beyond the thickness over which tunneling through this kind of medium can be expected to be efficient. However, systematic studies of the electron transport characteristics of bR-containing monolayers (or, for that matter, of single bR or PM units) were hampered by the difficulty to find a reliable, reproducible experimental system that allows such measurements. Monolayers of PM patches are problematic because of the practical difficulty in capturing and holding such patches between two electrodes and to prepare monolayers with sufficiently high coverage. Conducting probe atomic force microscopy (AFM) of a single PM patch is complicated because of the small contact area (leading to very low currents; see below) and the problem of making contact reproducibly. To date, only a few reports about current flow through PM in dry systems, namely for PM multilayers (9) and as patches (10), have appeared. The underlying origins or mechanisms have not been addressed.

We find that reconstituting bR in lipid bilayers on a solid, electrically conducting support provides a reliable basis for reproducible electronic transport measurements. We prepared such samples by vesicle formation and subsequent fusion. To form planar metal–protein–metal junctions we used the "lift-off, float-on" (LOFO) technique (11) as a "soft," nondestructive way to deposit gold contacts (60 nm thick, 2.10^{-3} cm^2) on the monolayer. The resulting structures are sufficiently robust to allow repeated and reproducible electron transport studies at ambient condition and room temperature. We used monolayers of native, apo-membranes as well as membranes with artificial bR pigments derived from synthetic retinal analogs. Structures of native *all-trans* retinal and the "locked" analogues used in this study are shown in Scheme 1. Based on our results with the modified bR samples, we conclude that transmembrane electron transport occurs essentially only via bR and not via the lipid bilayer and requires the presence of retinal or a similar π-electron system in the protein.

Results and Discussion

A suspension of PM fragments containing wild-type bR was prepared (12) and reconstituted with exogenous egg phosphatidylcholine (PC) into vesicles by a modification of the method of Racker (13). To further check protein-amount-dependent current–voltage (*I–V*) characteristics, another vesicular bR suspension was prepared by using octylthioglucoside (OTG) as a detergent (14). Monolayers of the native bR-containing membranes were then prepared by adsorbing the vesicles on an Al substrate (an ≈50-nm-thick film of Al evaporated on quartz) with a layer of natural aluminum oxide on its surface (represented here as AlOx). The attached vesicles then open and fuse, forming solid-supported lipid bilayers. To promote electrostatic adsorption of the vesicles, we first silanized the substrate surface with (3-aminopropyl)trimethoxysilane (APTMS) (15), followed by treatment with 0.1 M HCl, to obtain a positively charged surface. Both bR/PC or bR/OTG vesicle suspensions showed light-induced inward proton pumping as was

Conflict of interest statement: No conflicts declared.

This paper was submitted directly (Track II) to the PNAS office.

Abbreviations: bR, bacteriorhodopsin; PM, purple membrane; AFM, atomic force microscopy; LOFO, lift-off, float-on; PC, phosphatidylcholine; OTG, octylthioglucoside; APTMS, (3-aminopropyl)trimethoxysilane; *I–V*, current–voltage; BO, bacterioopsin.

†To whom correspondence may be addressed. E-mail: mudi.sheves@weizmann.ac.il or david.cahen@weizmann.ac.il.

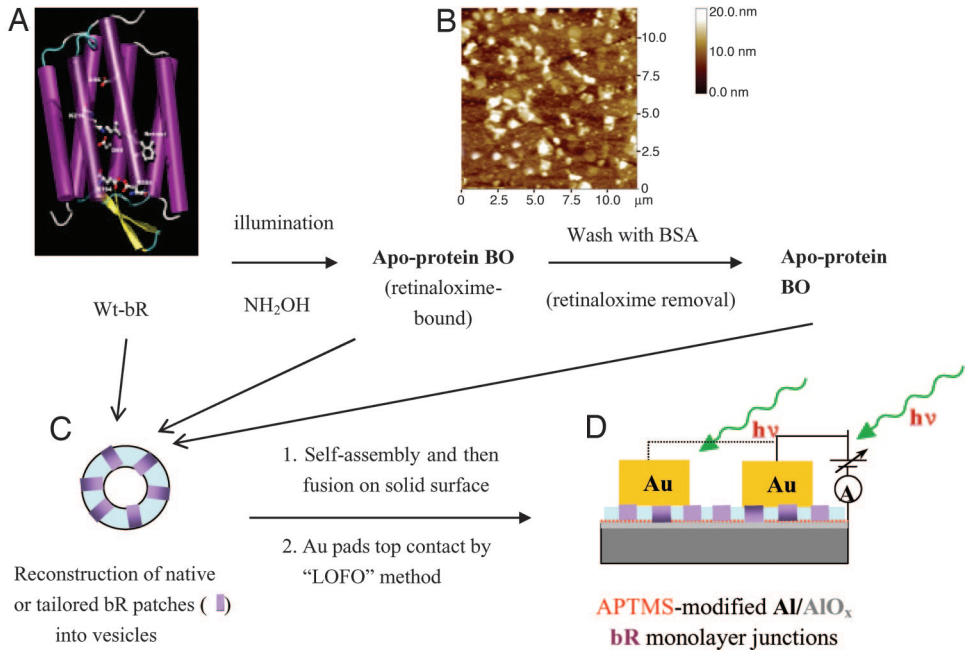

Fig. 1. Scheme of bR chemical tailoring and of the metal–protein–metal junction preparation. (*A*) Schematic representation of the 3D structure of bR. The seven α-helical domains form a transmembrane pore. The retinylidene residue is linked to the protein moiety via a protonated Schiff base linkage to Lys-216. (*B*) Representative AFM image (12 × 12 μm) of native bR patches prepared by 5 min of adsorption on an Al/AlOx substrate derivatized with APTMS. (*C*) Schematic of bR-containing vesicle. (*D*) Schematic of a Au/(single-bR-layer)/(APTMS-on-AlOx)/Al junction and measuring scheme.

found previously (13, 16). Based on this observation, we postulate a preferential orientation of bR with the cytoplasmic side facing the substrate surface after vesicle fusion to form bR monolayer membranes, consistent with orientation-dependent transmembrane proton translocation (17).

Fig. 2*A* shows a representative AFM image of a substrate, covered by bR-containing fused vesicle membranes, prepared by 10-min adsorption on the substrate. Because it is difficult to get an ideal monolayer (100% coverage), there are always some sample-free cracks or pinholes (typically tens of nanometers), between fused vesicle membranes. These cracks and pinholes are small enough for the Au pad (0.5-mm diameter) to bridge them (for transport measurement) but large enough for our AFM measurements to make thickness measurements possible. Section analysis shows the highest average height feature to be ≈5.2 nm, which agrees well with the thickness of a single PM patch, indicating the formation of a bR monolayer. The few white dots in Fig. 2*A* are left-over flattened vesicles on top of the film. Denser bR monolayer-containing membranes (Fig. 2*B*) result after ≈20-min adsorption of the vesicles on the substrate. Fig. 2*B* also allows a fortuitous measurement of the membrane/monolayer thickness (5.1 nm between markers) because of a crack in the membrane as a result of excessive drying. Longer adsorption times (>30 min) led to multilayer formation. Monolayers of membranes with modified bR were prepared by using the same procedures. All samples for electrical transport measurements were prepared by 20 min of adsorption and checked by AFM to assure monolayer quality. It is worth mentioning that, unlike surface-supported pure lipid bilayers, which are unstable and will disintegrate upon drying (let alone drying under N_2 flow) due to loss of hydrophobic interactions between lipids in dry state, the as-prepared PC/bR membranes are rather stable (even after mild N_2-drying), as revealed by AFM images. We ascribe this phenomenon to the high negative charges on bR surfaces, which can interact strongly with the positively charged substrate surface and act as a scaffold to stiffen the lipid bilayers. This interaction makes the bilayers sufficiently robust to allow repeated and reproducible electron transport studies in monolayer fashion under ambient conditions and at room temperature.

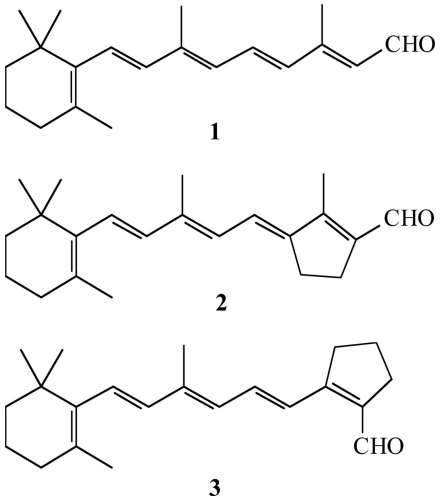

Scheme 1. Structures of *all-trans* retinal (native) (**1**), *all-trans*-locked (**2**), and *13-cis*-locked (**3**) analogues.

I–V measurements were carried out on planar junction structures in a class-10000 clean room at 293K and 40% relative humidity, with the sample sandwiched between the Al/AlOx substrate and the Au contacts. On each sample, several small, 0.5-mm-diameter Au pads were deposited on the monolayer by the LOFO technique. The circuit is completed by gently placing a tungsten electrode on the gold electrode (11). The main advantage of using the LOFO technique to prepare top contact, as compared with metal evaporation deposition or mercury contacts, is that the preformed metal patches can float on and span some small pinholes and cracks (typically in tens of nanometers), making electrical measurements successful. Fig. 3*A* shows typical *I–V* characteristics of a resulting

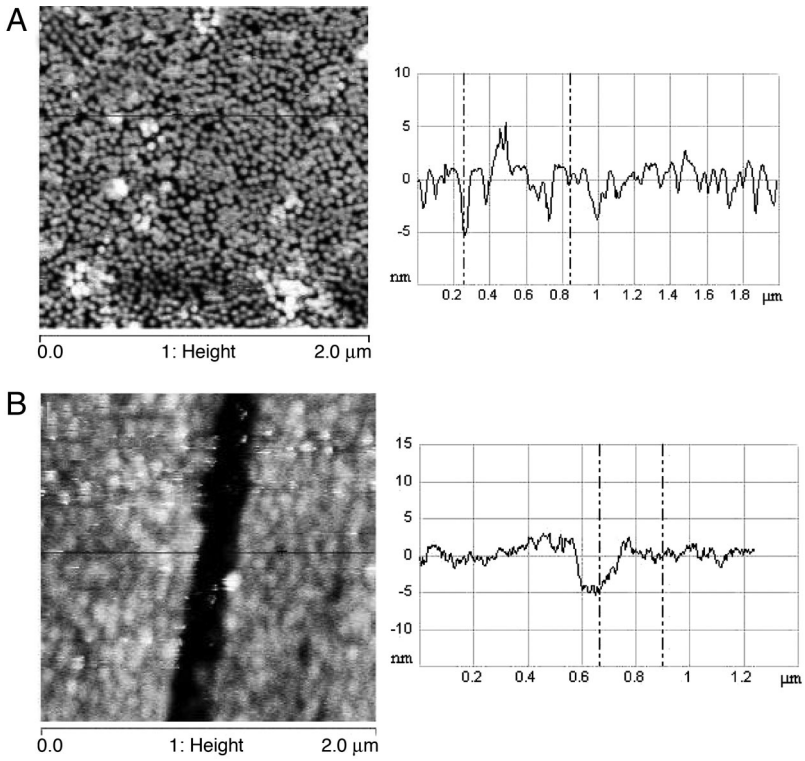

Fig. 2. AFM images of bR-containing fused membranes. (*A Left*) Representative AFM images (2×2 μm) of monolayers of fused membranes of bR-containing vesicles, prepared by 10-min adsorption on Al/AlOx substrate, derivatized with APTMS. (*A Right* and *B Right*) Line scans showing an average height of the strongest features of ≈5.2 nm. The height bar covers 20 nm. (*B Left*) A more densely packed bR containing a monolayer, prepared by 20-min adsorption of vesicles on the substrate (1.25- $\times$ 1.25-μm image). The crack in the membrane, induced by excessive drying (something that was carefully avoided in the preparation of the samples used for electrical transport measurements) shows the monolayer to be 5.1 nm thick (between markers).

metal/(bR monolayer-in-lipid bilayer)/metal junction over a ±1-V bias range. The *I–V* curves were recorded after dark equilibration followed by irradiation with green ($\lambda > 550$ nm, 20 mW/cm^2) light. In the dark, 0.75 nA flows at a 1-V applied bias was detected. After steady-state illumination with green light, the current increases from 0.75 to 1.7 nA at a 1-V applied bias. Once the green light was blocked, the current decayed over 2–3 min to its original dark value. Possibly, the light effect is associated with the formation of the photochemically induced M intermediate that may well have a slower thermal decay under dry monolayer conditions than in membranes in solution (18). The system can be cycled between these two states by alternating green light and dark adaptation, indicating that the bR preparation retains its photoactivity. Control devices with only an APTMS monolayer incorporated between Al/AlOx and Au contacts were always shorted with typical junction resistances <50 Ω, indicating that the AlO_x layers are thin enough for reliable electrical measurements.

The crucial role that bR plays in producing the measured transmembrane currents is illustrated by using another monolayer membrane with higher bR content, which was prepared as reported in ref. 14 by using OTG as a detergent for bR vesicle formation. These two kinds of bR monolayer (containing membranes with different bR contents prepared from bR/PC or bR/OTG vesicles) will be noted as membrane A or B and junction A or B for corresponding junctions. The typical absorbances (in OD) at ≈560 nm are $\approx 0.15 \times 10^{-3}$ and $\approx 1.0 \times 10^{-3}$ for membrane A and B, respectively. The bR content of membrane B (≈6-fold higher than that of membrane A) is similar to

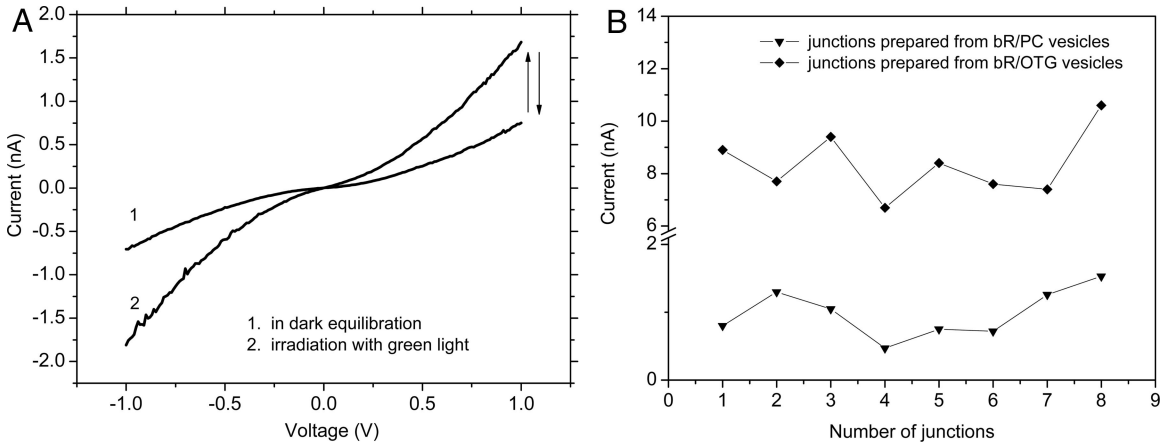

Fig. 3. *I–V* characteristics of metal–(bR monolayer)–metal junctions. (*A*) *I–V* curves of a Au/(wild-type bR)/(APTMS–AlOx–Al) junction containing oriented bR monolayer, prepared by vesicle fusion and measured at ambient conditions in the dark, upon illumination at $\lambda > 550$ nm, and dark adaptation. The arrows show that the *I–V* responses can be cycled between the two states. The Au pad area was 2.10^{-3} cm^2. (*B*) Plot of dark currents at a +1.0-V bias voltage for eight independent junctions prepared from bR/PC vesicles and from bR/OTG vesicles, respectively.

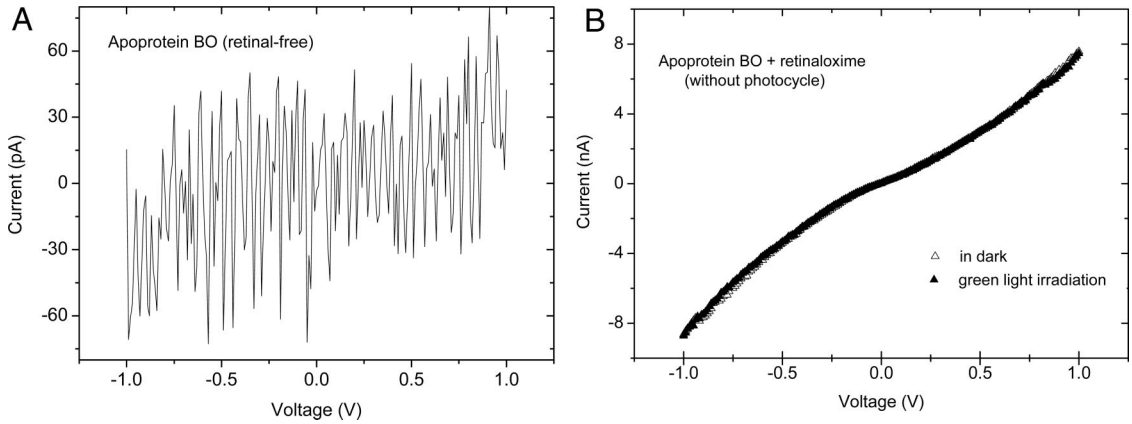

Fig. 4. *I–V* characteristics of metal–apo-membrane–metal junctions. (*A*) Typical *I–V* characteristic of a Au/apo-membrane (retinal-free)/(APTMS–AlOx–Al) junction prepared by vesicle fusion and measured at ambient conditions. (*B*) *I–V* curves of Au/apo-membrane (apo-protein bR plus retinaloxime)/(APTMS–AlOx–Al) junction prepared by vesicle fusion and measured at ambient conditions in the dark and upon illumination at $\lambda > 550$ nm. No photoeffect on the junction current was observed.

that of bR in a dry PM monolayer, based on both the experimental absorbance (18) and the value, calculated for an ideal PM monolayer ($\approx 1 \times 10^{-3}$ OD at $\approx$560 nm). Averaged dark currents at a given applied bias of junctions B are nearly eight times those found with junctions A, i.e., very closely proportional to the bR content in the membranes (Fig. 3*B*). This finding suggests that electrons pass mainly via bR through the membrane rather than through the lipid bilayers. Both junctions A and B are photoactive and, when normalized to bR content, show similar *I–V* characteristics.

The average light effects on the current flow of junctions A and B are typically $\approx$1 and $\approx$3 nA at a 1-V applied bias, respectively. The light-induced change in junction B current is somewhat lower than expected, based on the bR contents of the two types of samples. The difference might be due to differences in the fractions of the M intermediate that can accumulate in samples A and B and/or with differences between the two samples in the photo-induced protein conformation change, imposed by M formation.

Measurable current flow through the 5-nm-thick protein is remarkable, as compared with other similar systems with same gap. For instance, we note that a typical 1-nm-long peptide will pass $\approx$12 nA at 0.5 V (19), similar to that passed by a single 1.2-nm-long octane dithiol (20). All other factors being equal and assuming an exponential decrease in (tunnel) current with increasing molecule length, yields a current of $\approx 10^{-23}$ A for an $\approx$35-nm^2 area (equivalent to the area of one bR trimer plus lipids), using the Simmons model for direct tunneling (compare section 2 and figure 2 in ref. 21). Based on our optical absorption data, we estimate the density of bR in our membranes to be $\approx 10^9$ bR trimer per 0.002-cm^2 junction. This value translates into an experimentally measured current of 3×10^{-19} A per bR trimer, i.e., at least four orders of magnitude more than what is estimated for direct tunneling through 5-nm peptides, alkyls, or a dielectric medium with similar dielectric constant. It is therefore likely that the process of current transport is more complex than straightforward tunneling through a single barrier. Indeed, natural proteins whose function involves electron transfer often need to transfer electrons with high directional specificity over large distances. Such transfer over longer distances always involves a chain of cofactors, such as redox centers (22). In analogy to these redox centers, we can consider retinal, the π-electron system that is in the center of bR, as an intermediate on the path of the electrons through the protein. If, instead of tunneling through one long molecule, the process occurs in (at least) two steps, with a delocalized electron way-station 2.3 nm from each side, estimates similar to those used above give currents of $\approx 10^{-20}$ A per 35 nm^2 (21).

To check this last idea experimentally, we prepared and examined junctions of retinal-free bR membranes. To prepare these membranes, we first illuminated the protein mixed with hydroxylamine. This reaction leads to breaking the protonated Schiff base bond, yielding the apo-protein bacterioopsin (BO) and retinaloxime, which remains attached to the membrane (12). The retinaloxime was then removed by resuspending the apo-membranes in a solution of BSA, followed by incubation and centrifugation. BSA competitively solubilizes the retinaloxime that is embedded within the membrane. Repeated centrifuge washes remove BSA once the protein has been purified of all chromophore contaminants (5). Current flow through the (retinal-free) apo-membrane is approximately three orders of magnitude lower than was observed with native bR membranes (compare Figs. 4*A* and 3*A*). The current was very noisy and unstable. This result supports the idea that current flows dominantly through the bR proteins and that the retinal serves as a current transport mediator. Furthermore, the photo-effect observed with the native bR-containing membranes can be ascribed to the retinal.

To check whether the retinal–protein covalent bond is a prerequisite for electron transport, we measured apo-membrane samples containing retinaloxime. At least part of the retinaloxime will still occupy the retinal-binding site as deduced from CD spectroscopy (23). *I–V* curves of such samples showed behavior similar to that of native bR in terms of current magnitude, but they did not show any response to green light as expected in samples lacking absorption in this region (Fig. 4*B*). The *I–V* characteristics are closer to linear than what we find for wild-type samples, which may indicate a change of tunneling gap between retinal and retinaloxime.

To shed further light on the effect of retinal isomerization and the photocycle on the light effect, we studied artificial pigments derived from *13-cis* (**3**)-locked [or *all-trans* (**2**)-locked] retinals (Scheme 1), where the critical $C_{13}{=}C_{14}$ isomerization is blocked by a 5-membered ring structure (24, 25). *I–V* characteristics similar to those obtained with apo-membranes with retinal oxime are found for those artificial pigments. The lack of photoeffect in junctions made with apo-membranes is in keeping with the absence of a photocycle in these samples (24, 26), supporting the hypothesis that occurrence of retinal isomerization is a prerequisite for the light effect. We assume that no pronounced, electric-field-induced, bR conformational change occurs (i.e., bR will remain native-like) in the $\leq 10^6$ V/cm fields

across the protein that are reached in our experiments. We note that the Au top electrode is semitransparent for green light. For example, a 55-nm Au film transmits ≈70% at ≈550 nm (27). A possible physical origin of the photoeffect from the nanogap, planar, metal nanostructure itself, for example by surface plasmon excitation, can be safely ruled out (28). On the basis of these and the above described results, we ascribe the photoeffect on the junction currents to the *13-cis/all-trans* retinal photoisomerization (4) and the protein conformational changes that result from it. We note that in our experiments the electrons originate from metal electrodes and pass through bR from electrode to electrode under applied voltage, with bR acting as an electronic conduction medium. In this respect, bR differs from systems like the photosynthetic reaction centers, in which electron transfer between cofactors is photoinduced.

It is clear from the calculations and from, for example, the negative result of Fig. 4*A* that the mechanism is not (only) one of direct tunneling. It is also unlikely to be (solely) one of hopping in view of the (single molecule) results of the work of Selzer *et al.* (29). How then can the electrons cross the protein? Our experimental results clearly indicate that the retinal chromophore is a necessary component for the conduction process. It is well known that the retinal is connected to the extracellular side via a H-bonded network, which probably provides an electrostatically screened path for charge transport. Because there also is good coupling between the retinal and extracellular side in the dark, this path must be present irrespective of illumination. Its presence can explain the higher-than-expected currents that we measure. The connection of the retinal to the cytoplasmic surface is known to be light-activated, which may explain the light effect that we observe. Both of these suggestions need further investigation.

The importance of charge transfer between the retinal chromophore and the protein environment for bR in its ground state was suggested, based on theory, by Sakai *et al.* (30). These authors hypothesized that the chromophore is stabilized in bR by an interaction of its highest occupied and lowest unoccupied molecular orbitals with the protein environment. If sufficient charge is transferred between two sites, due to the strong highest occupied–lowest unoccupied molecular orbital interaction, the (π-conjugated) chromophore can be viewed as a one-electron-reduced/-oxidized species (if it behaves as an electron acceptor/donor). The most probable chromophore–protein interaction was calculated to be via the H-bonded network along the presumed proton pathway.

It is also tempting to suggest that proton-coupled electron transport (22, 31) plays a role because there are quasi one-dimensional protonated water chains in the proton channel of bR (32, 33) embedded in solid supported lipid bilayers, which will be normal to the two electrodes in our set-up (17). This suggestion may explain part of the difference between electron transport through bR and through supposedly water-free peptides. In view of such a situation several questions arise.

1. How much, if at all, can electron transport through bR benefit from a built-in proton channel?
2. How will the chromophore and the intervening protein structure affect the rate of long-range electron transport?
3. To what extent can bound water molecules inside bR contribute to the electronic current?

Possibly, temperature-dependent *I–V* measurements, although these are far from trivial with this system, can shed light on these issues.

We note that, unlike the case for a bR monolayer in solution, the Faradaic photocurrent of a dry bR monolayer originating from transmembrane proton translocation is negligible compared to the observed junction currents because the proton source is limited. Our finding that all observed junction currents (in dark or under green light) are zero, within experimental error [≈10 pA (compare Fig. 4*A*)], supports the absence of steady-state proton translocation. There is, therefore, no measurable photoresponse between approximately ±30 mV at ≈0 V (*cf.* ref. 34; any ≤15- to 20-mV photovoltage is in the noise of our measurement), indicating that light-driven proton translocation across the bR monolayer held between the electrodes contributes negligibly to the steady-state light currents. This conclusion was confirmed by the proton-translocation-induced bR photocurrents in similar solid-supported lipid bilayers (typically 4–8 nA/cm^2) (18) that are two to three orders of magnitude lower than the junction currents that we measure here (≈0.5–5 μA/cm^2). Still, even without any direct connection between proton and electron transport, we note that a protein that, from the point of electrostatics (screening), is suitable for proton transfer, may well be able to use the same mechanism of screening to facilitate electron transport.

We can also compare our results with the previously reported photocurrents through the ≈500-nm (8) and ≈100-μm (9) dry multilayers by calculating values per PM monolayer (5 nm). Such normalization yields values of ≈0.01 nA per single PM layer per cm^2, i.e., some four to five orders of magnitude less than the junction currents that we measure here (≈0.5–5 μA/cm^2). This dramatic difference illustrates the difficulty in interpreting the earlier, pioneering measurements (9) and stresses the importance of using as well defined a configuration as possible for electron transport measurements of biological systems. With such configurations, it then also becomes possible to make measurements as a function of controlled variations of the system.

Conclusion

We have shown that reconstituting bR in lipid bilayers on an electrically conducting solid support via vesicle fusion tactics, followed by top contact realized by using the LOFO technique, is a reliable basis for reproducible electronic transport measurements. *I–V* measurements and theoretical calculations together reveal that electrons transfer through the protein more than four orders of magnitude faster than would be estimated for direct tunneling through 5-nm, water-free peptides. Based on our results with the modified bR samples, we conclude that transmembrane electron transport occurs essentially only via bR and not via the lipid bilayer and requires the presence of retinal or a similar π-electron system in the protein. The junctions show photoconductivity as long as the retinal can isomerize, as a result of light absorption. The contribution of light-driven proton ejection to the steady-state photocurrents is negligible.

Apart from the fact that we succeeded in building a sturdy planar metal–protein–metal junction that presents a relatively straightforward, dry experimental system for systematic current-transport measurements, our results pose a fascinating question: If bR can transport (and transfer) electrons, why don't we find such a function in nature? Is it because electron transfer was too inefficient and, thus, was eliminated by evolution, or is our finding a strictly nonbiological one? Even without biological relevance (or if any biological processes are hidden so well that we have not found them), we have shown here that bR presents a relatively simple and stable biological system to explore electronic transport with a biological material that can be manipulated with all of the tools know to modern chemistry and biology.

Materials and Methods

Preparation of PM and Artificial Pigments. A suspension of PM fragments containing wild-type bR was prepared by a standard method (12). The apo-membrane was prepared from bR by reaction with hydroxylamine according to a previously described method (35). This chemical reaction results in the breakage of the Schiff base bond and yields the apo-protein BO and retinaloxime, which remains attached to the membrane (12). Removal of the retinaloxime was thereafter accomplished by

resuspending the apo-membranes in a solution of BSA, followed by incubation and centrifugation. The process was repeated five times.

Artificial pigments were prepared by reconstituting the apo-membrane (suspension in water) with trans-locked and *13-cis*-locked retinal analogs (24, 25), respectively. Briefly, reconstitution was performed by the addition of 25–28 nmol of the retinal analogs and dissolved in 5–10 μl of 2-propanol, to yield a 1-ml aqueous suspension of 32 nmol of apo-membrane.

Preparation of bR-Containing Vesicles and Fused Membranes. Reconstitution of PM fragments or various artificial pigments with exogenous egg PC into vesicles was carried out by a modification of the method of Racker (13). Briefly, 10 mg of egg PC was dispersed in 2 ml of 150 mM KCl solution (pH 9.2) with 0.5 mg wild-type bR or various artificial pigments by vortex shaking. The multilayered liposomes were transferred to a sonication vessel and sonicated with a tip 30 times for 10 sec, with 50-sec intervals in an ice bath to get unilamellar vesicles. The vesicles with high bR content were prepared by following the procedure of Kouyama *et al.* (14). Briefly, after washing with 0.17% Tween 20 in the presence of 0.16 M NaCl and 10 mM Hepes (pH 8.0) for 30 min, the PM (5 mg/ml) was vesicularized by incubating at 32°C for 5–7 days with 6.7 mM OTG in the presence of 1 M ammonium sulfate (AS) and 0.4 M NaCl at pH 6.4 (maintained by phosphate buffer). After the incubation period, the samples were centrifuged at $1,000 \times g$ for 40 min to remove the formed precipitate of irregularly stacked membranes. To remove the excess OTG and electrolytes from the vesicular bR suspensions, the suspensions were dialyzed in two stages against electrolyte solutions of lower concentrations: (*i*) 0.5 M AS and 0.05 M phosphate buffer, pH 6.4, and (*ii*) 0.1 M AS and 0.01 M phosphate buffer, pH 6.4. The suspension was kept on a shelf before use. The inside-out orientation of the vesicles was confirmed by checking the proton pump activity (measured by the pH change (alkalinization) of the outside medium on green-light illumination).

For preparing bR (or artificial bR pigment) monolayer-containing membrane, an APTMS-monolayer-modified (15) aluminum substrate (an ≈50-nm-thick Al film evaporated on quartz with an Al_2O_3 surface layer) was immersed into 0.1 M HCl for 30 sec to get a positively charged surface. The modified substrate was then immersed into vesicular suspension for ≈10–30 min, then transferred into Tris buffer solution, pH 9.2, and was incubated for >3 h to ensure vesicle fusion. After sonicleaning in a bath for ≈2 min, the sample was dried by nitrogen and ready for characterizations.

Junction Preparation. The planar junction structures were completed by applying a second electrode onto the membrane adsorbed on the Al surface. Therein gold top contacts were deposited on the membrane surface in a very soft manner using the LOFO technique (11). Au dots (60 nm thick and 0.5 mm in diameter) were evaporated onto clean glass slides, from which they were allowed to peel by dipping the slide at an angle in 2% (vol/vol) solution of HF in water. The slide was then dipped into pure water containing the modified Al substrates to allow the Au leaves to float. The bR-modified Al substrates were then lifted with Au pads on top, and the samples were dried at room temperature under a very mild N_2 stream.

Instruments. *I–V* characteristics were measured with a W needle connected to a micromanipulator to contact the Au pad [an InGa drop on the Au minimizes mechanical (pressure) damage to the film], and an Hewlett–Packard 4155 semiconductor parameter analyzer in the voltage scan mode; these measurements were made at ambient conditions.

AFM topographic images were acquired in tapping mode under ambient conditions (Nanoscope IIIa; Digital Instruments, Santa Barbara, CA) using a standard silicon nitride cantilever. The UV/visual light absorption spectra of bR monolayer membrane on quartz glass were recorded in the dark or under green-light illumination with a 8540 diode-array spectrophotometer (Hewlett–Packard). In this work, the green and blue lights were obtained with a tungsten–halogen light source and the combination of a cut-off filter ($\lambda > 550$ nm for green light and 380 nm $< \lambda <$ 440 nm for blue light) and a heat filter.

We thank the reviewers for constructive criticism. This work was supported by the Israel Ministry of Science's Tashtyoth Program, the Ilse Katz Centre for Materials, and the Kimmel Centre for Nanoscale Science. Y.J. was supported by a Norman Sosnow Foundation postdoctoral fellowship. M.S. holds the Katzir–Makineni Chair in Chemistry, and D.C. holds the Schaefer Chair in Energy Research.

1. Oesterhelt, D. & Stoeckenius, W. (1971) *Nat. New Biol.* **233,** 149–152.
2. Henderson, R. & Unwin, P. N. T. (1975) *Nature* **257,** 28–32.
3. Lanyi, J. K. (2004) *Mol. Membr. Biol.* **21,** 143–150.
4. Pettei, M. J., Yudd, A. P., Nakanishi, K., Henselman, R. & Stoeckenius, W. (1977) *Biochemistry* **16,** 1955–1959.
5. Birge, R. R., Gillespie, N. B., Izaguirre, E. W., Kusnetzow, A., Lawrence, A. F., Singh, D., Song, Q. W., Schmidt, E., Stuart, J. A., Seetharaman, S. & Wise, K. J. (1999) *J. Phys. Chem. B* **103,** 10746–10766.
6. Crittenden, S., Howell, S., Reifenberger, R., Hillebrecht, J. & Birge, R. R. (2003) *Nanotechnology* **14,** 562–565.
7. Jussila, T., Li, M. L., Tkachenko, N. V., Parkkinen, S., Li, B. F., Jiang, L. & Lemmetyinen, H. (2002) *Biosens. Bioelectron.* **17,** 509–515.
8. Manoj, A. G. & Narayan, K. S. (2003) *Appl. Phys. Lett.* **83,** 3614–3616.
9. Xu, J., Bhattacharya, P., Marcy, D. L., Stuart, J. A. & Birge, R. R. (2001) *Electron. Lett.* **37,** 648–649.
10. García, R., Tamayo, J., Soler, J. M. & Bustamante, C. (1995) *Langmuir* **11,** 2109–2114.
11. Vilan, A., Shanzer, A. & Cahen, D. (2000) *Nature* **404,** 166–168.
12. Oesterhelt, D. & Stoeckenius, W. (1974) *Methods Enzymol.* **31,** 667–678.
13. Racker, E. (1973) *Biochem. Biophys. Res. Commun.* **55,** 224–230.
14. Denkov, N. D., Yoshimura, H., Kouyama, T., Walz, J. & Nagayama, K. (1998) *Biophys. J.* **74,** 1409–1420.
15. Jin, Y. D., Kang, X. F., Song, Y. H., Zhang, B. L., Cheng, G. J. & Dong, S. J. (2001) *Anal. Chem.* **73,** 2843–2849.
16. Kouyama, T., Yamamoto, M., Kamiya, N., Iwasaki, H., Ueki, T. & Sakurai, I. (1994) *J. Mol. Biol.* **236,** 990–994.
17. Steinem, C., Janshoff, A., Höhn, F., Sieber, M. & Galla, H.-J. (1997) *Chem. Phys. Lipids* **89,** 141–152.
18. He, T., Friedman, N., Cahen, D. & Sheves, M. (2005) *Adv. Mater.* **17,** 1023–1027.
19. Xiao, X. Y., Xu, B. Q. & Tao, N. J. (2004) *J. Am. Chem. Soc.* **126,** 5370–5371.
20. Xu, B. Q. & Tao, N. J. J. (2003) *Science* **301,** 1221–1223.
21. Salomon, A., Cahen, D., Lindsay, S., Tomfohr, J., Engelkes, V. B. & Frisbie, C. D. (2003) *Adv. Mater.* **15,** 1881–1890.
22. Page, C. C., Moser, C. C., Chen, X. X. & Dutton, P. L. (1999) *Nature* **402,** 47–52.
23. Becher, B. & Cassim, J. (1977) *Biophys. J.* **19,** 285–297.
24. Chang, C. H., Govindjee, R., Ebrey, T., Bagley, K. A., Dollinger, G., Eisenstein, L., Marque, J., Roder, H., Vittitow, J. & Fang, J. M. (1985) *Biophys. J.* **47,** 509–512.
25. Aharoni, A., Ottolenghi, M. & Sheves, M. (2002) *Biophys. J.* **82,** 2617–2626.
26. Delaney, J. K., Brack, T. L., Atkinson, G. H., Ottolenghi, M., Steinberg, G. & Sheves, M. (1995) *Proc. Natl. Acad. Sci. USA* **92,** 2101–2105.
27. Xiao, M. F. & Rakov, N. (2003) *J. Phys. Condens. Matter* **15,** L133–L137.
28. Jin, Y. D. & Friedman, N. (2005) *J. Am. Chem. Soc.* **127,** 11902–11903.
29. Selzer, Y., Cabassi, M. A., Mayer, T. S. & Allara, D. L. (2004) *J. Am. Chem. Soc.* **126,** 4052–4053.
30. Sakai, K., Vacek, G., Lüthi, H. P. & Nagashima, U. (1997) *Photochem. Photobiol.* **66,** 532–540.
31. Murgida, D. H. & Hildebrandt, P. (2001) *J. Am. Chem. Soc.* **123,** 4062–4068.
32. Nagle, J. F. & Morowitz, H. J. (1978) *Proc. Natl. Acad. Sci. USA* **75,** 298–302.
33. Rousseau, R., Kleinschmidt, V., Schmitt, U. W. & Marx, D. (2004) *Phys. Chem. Chem. Phys.* **6,** 1848–1859.
34. Crittenden, S., Reifenberger, R., Hillebrecht, J., Birge, R., Inerowicz, D. & Regnier, F. (2005) *J. Micromech. Microeng.* **15,** 1494–1497.
35. Oesterhelt, D., Schumann, L. & Gruber, H. (1974) *FEBS Lett.* **44,** 257–261.